Schicks, J., Strauch [Beeskow-Strauch], B., Heeschen, K., Spangenberg, E., Luzi-Helbing, M. (2018): From Microscale (400 µl) to Macroscale (425 L): Experimental Investigations of the CO2/N2-CH4 Exchange in Gas Hydrates Simulating the Iġnik Sikumi Field Trial. - *Journal of Geophysical Research*, *123*, 5, pp. 3608—3620.

DOI: http://doi.org/10.1029/2017JB015315

Journal of Geophysical Research: Solid Earth

RESEARCH ARTICLE
10.1029/2017JB015315

Special Section:
Gas Hydrate in Porous Media: Linking Laboratory and Field Scale Phenomena

From Microscale (400 μl) to Macroscale (425 L): Experimental Investigations of the CO_2/N_2-CH_4 Exchange in Gas Hydrates Simulating the Iġnik Sikumi Field Trial

J. M. Schicks[1], B. Strauch[1], K. U. Heeschen[1], E. Spangenberg[1], and M. Luzi-Helbing[1]

[1]GFZ German Research Centre for Geosciences, Potsdam, Germany

Key Points:
- When exposed to a CO_2-N_2 gas mixture (23 mol%/77 mol%), no replacement of the hydrate-bonded CH_4 with CO_2 or N_2 could be observed
- Chemical environment changes due to CO_2-N_2 injection led to two processes: dissociation of initial hydrate and formation of a mixed hydrate
- The dissociation of the CH_4 hydrate occurs at pressures within the CH_4 hydrate stability field and increases with decreasing pressure

Correspondence to:
J. M. Schicks,
schick@gfz-potsdam.de

Citation:
Schicks, J. M., Strauch, B., Heeschen, K. U., Spangenberg, E., & Luzi-Helbing, M. (2018). From microscale (400 μl) to macroscale (425 L): Experimental investigations of the CO_2/N_2-CH_4 exchange in gas hydrates simulating the Iġnik Sikumi Field Trial. *Journal of Geophysical Research: Solid Earth*, *123*, 3608–3620. https://doi.org/10.1029/2017JB015315

Received 4 DEC 2017
Accepted 23 APR 2018
Accepted article online 4 MAY 2018
Published online 24 MAY 2018

Abstract In 2012 the production of CH_4 from hydrate-bearing sediments via CO_2 injection was conducted in the framework of the Iġnik Sikumi Field Trial in Alaska, USA. In order to preserve the injectivity by avoiding a formation of CO_2 hydrate in the near-well region, a mixture containing 77 mol% N_2 and 23 mol% CO_2 was chosen. The interpretation of the complex test results was difficult, and the nature of the interaction between the N_2-CO_2 mixture and the initial CH_4 hydrate could not be clarified. In this study we present the results of our experimental investigations simulating the Iġnik Sikumi Field Trial at different scales. We conducted (1) in situ Raman spectroscopic investigations to study the exchange process of the guest molecules in the hydrate phase on a molecular level in a flow-through pressure cell with a volume of 0.393 ml, (2) batch experiments with pure hydrates and hydrate-bearing sediments in pressure cells with volumes of 420 ml, and (3) the injection of a CO_2-N_2 mixture into a hydrate-bearing sediment in a large-scale reservoir simulator with a total volume of 425 L. The results indicate a dissociation of the initial CH_4 hydrate rather than an exchange reaction. The formation of a secondary mixed hydrate phase may occur, but this process strongly depends on the local composition of the gas phase and the pressure at given temperature.

1. Introduction

Enormous amounts of CH_4 are bonded in natural gas hydrates occurring at all active and passive continental margins, in permafrost regions, and deep lakes (Kvenvolden & Lorenson, 2001). CH_4 is encased as guest molecule in the three-dimensional network of hydrogen-bonded water molecules forming cavities of different sizes. To produce the CH_4 from these ice-like crystalline solids, different approaches such as depressurization as well as thermal and chemical stimulation have been tested not only in laboratory studies but also in field trials (e.g., Boswell et al., 2017; Dallimore & Collett, 2005; Yamamoto et al., 2014). Using the injection of CO_2 into hydrate-bearing sediments as a chemical stimulation method appears to be particularly favorable because it is supposed to combine the release of CH_4 from the hydrate phase with the storage of CO_2 into the solid hydrate. Therefore, several experimental and modeling studies in the last decade focused on this approach (Zhao et al., 2012, and literature within). Depending on the experimental conditions, the amount of CH_4 recovered from a hydrate phase due to CO_2 replacement varied from 15% in 800 hr (Hirohama et al., 1996) to 50% within 5 hr (Lee et al., 2003) to 60% in 300 hr (Kvamme et al., 2007), to give just few examples. It could be shown that the exchange of CH_4 with CO_2 initially takes place at the surface of the hydrate grain and goes along with a partial opening or rearrangement of the cavities (Falenty et al., 2016; Ota et al., 2005; Schicks et al., 2011). Laboratory experiments usually avoid free pore water that may transform into CO_2 hydrate when CO_2 is injected resulting in a decrease of permeability and thus reduced injectivity or clogging. Such an undesired CO_2 hydrate formation close to the injection point could also be observed when supercritical CO_2 was injected into a cold reservoir (275 K) containing free pore fluid (salt water) besides CH_4 hydrate in a sediment matrix (Deusner et al., 2012). However, in natural systems, the hydrate saturation in the sediment is usually less than 100%, and a free water phase coexists besides the hydrate phase in the pore space. To avoid the formation of CO_2 hydrate with this residual water, the idea of injecting a CO_2-N_2 mixture rose. According to Kang et al. (2001) and Sfaxi et al. (2012), the pressure and temperature conditions for the formation of a CO_2-N_2-hydrate are shifted to higher pressure and lower temperatures compared to simple CO_2 hydrates. In other words, depending on the *p-T* conditions and the composition of the used N_2-CO_2 mixture, the formation of a hydrate phase with the residual water phase can be avoided. In addition, experimental results published by Park et al. (2006) and Koh et al.

(2012) indicate an enhanced recovery rate of CH_4 from the hydrate phase when a CO_2-N_2 mixture is used for the chemical stimulation instead of pure CO_2. In the framework of the Iġnik Sikumi Field Trial, a mixture of about 23 mol% CO_2 and 77 mol% N_2 was injected into the hydrate reservoir. The field trial was conducted within the Prudhoe Bay Unit on the Alaska North Slope during 2011 and 2012 (Boswell et al., 2017; Schoderbeck et al., 2013). The project aimed to determine the feasibility of gas injection into hydrate-bearing sediments and the observation of the reservoir response upon subsequent flowback in order to assess the potential for the exchange of CH_4 with CO_2 in the naturally occurring gas hydrate. The chosen area exhibits relatively massive and homogeneous sand units with a hydrate saturation of about 60–72%. As the primary testing interval, the "C-1 sand" layer in 684–693-m depth was selected. The reservoir conditions within this layer comprise a pressure of 6.9 MPa, a temperature of 278 K, and an average hydrate saturation of 72%. The field test was conducted in four steps (Boswell et al., 2017):

1. Injection (14 days): During this period, a total volume of 6,114 m^3 (215.9 Mscf) gas containing 22.5% CO_2 and 77.5% N_2 was injected into the reservoir. The injection pressure was held constant at 9.8 MPa, and the temperature of the injected medium remained within 0.1 K of the formation temperature of 278 K. At the early stages of the injection, a decrease in injectivity, probably due to hydrate formation, was observed.
2. Shut-in soak (2.5 days): Operational issues associated with the changeover from injection to production resulted in a period of shut-in time before the flowback could be started. During this time, the bottom-hole pressure dropped from 9.8 to 8.27 MPa.
3. Unassisted flowback (1.5 days): During the unassisted flowback, only gas but no water was produced to the surface. The produced gas mixture was continually monitored with a gas chromatograph. Boswell et al. (2017) reported that during this phase, CH_4 was the dominant gas, but they did not quantify the composition of the produced gas phase.
4. Jet-pumped assisted flowback (30 days): During the first 8 days of the jet-pumped assisted flowback, the pressure was kept above the destabilization pressure of the native CH_4 hydrate at a given temperature resulting in a relatively low and variable production of gas, water, and solid. During the next 2–3 days of jet-pumped assisted flowback, the pressure was reduced to pressures very close to the CH_4 hydrate stability pressure at reservoir condition. An increased production of gas with increasing content of CH_4 (above 80 mol%) was observed. The bottom-hole pressure during the third phase of the jet-assisted flowback was chosen below the predicted CH_4 hydrate stability conditions. The produced gas phase contained more than 95 mol% of CH_4.

A total of 24,410 m^3 (855 Mscf) of CH_4 was released during the production period. Seventy percent of the injected N_2 and 40% of the injected CO_2 were recovered, which implies that 1,421 m^3 (50.2 Mscf) of N_2 and 826 m^3 (29.2 Mscf) of CO_2 remained in the reservoir.

The results of the field test are quite complex and not easy to interpret. A slightly decreasing injectivity indicated the formation of additional hydrate with unknown composition in the reservoir. It is also not known if and how the composition of the native hydrate phase changed during the field trial. The investigation of the recovered gas indicates a preferential retention of CO_2 in the reservoir, but it is not clear if the CO_2 is bonded within the hydrate structures or only dissolved into the pore water. It also shows that CH_4 was released from the reservoir already during the unassisted flowback and during the jet-pumping flowback at pressures within the CH_4 hydrate stability field, but it is not clear whether the produced methane was derived from direct exchange with CO_2 in the hydrate structures. Likewise, it might be released as a result of other processes such as the dissociation of the native hydrate phase due to the chemical disequilibrium as a result of the CO_2-N_2 injection. The absolute amount of N_2 remaining in the reservoir is almost twice as much as the amount of the remaining CO_2, but it could not be clarified how the reservoir restrained the flowback of N_2.

With the present study, we aim to simulate the processes occurring during the Iġnik Sikumi Field Trial on different scales to understand at least the subprocesses of the complex interactions observed in the field test. We conducted experiments in pressure cells from 0.393 ml to 425 L. To determine changes in the composition of the hydrate phase, we used in situ Raman spectroscopy as well as ex situ X-ray diffraction and Raman spectroscopy. With the injection of the CO_2-N_2 mixture into a hydrate-bearing sediment in the LArge scale Reservoir Simulator (LARS), we aimed to understand the interaction of the CO_2-N_2 mixture with the CH_4 hydrates phase on a larger scale.

2. Materials and Methods

2.1. Microscale In Situ Measurements Using Raman Spectroscopy

In situ investigations of the interaction between the gas phase and the hydrate phase were conducted using Raman spectroscopy. For the Raman spectroscopic measurements, the initial CH_4 hydrate phase was synthesized from 150 μl deionized water and CH_4 (purity 2.5) in a pressure cell (0.393 ml) at 7 MPa. The method of initial hydrate formation has been described in detail elsewhere (Schicks & Ripmeester, 2004). The hydrate growth took place over several days at 7 MPa and 282.7 K until Raman spectroscopic measurements showed the characteristic spectra for a CH_4 hydrate throughout the solid phase (see Figures 1 and 3b) in coexistence with the gas phase. Since there was no liquid phase visible at that point, it was assumed that the water phase was completely transformed into a CH_4 hydrate phase.

The pressure cell could be used in a temperature range between 245 and 350 K and a pressure range between 0.1 and 10.0 MPa. The temperature of the sample cell was controlled by a thermostat and determined with a precision of ±0.1 K. A pressure controller adjusted the sample pressure with a precision of 2% relative. An important feature of the pressure cell was the use of a continuous gas flow of 1 ml/min, which allowed for the change of the gas composition during the ongoing measurements. The continuous gas flow was measured and regulated with a commercial flowmeter F230-FA-11-Z from Bronkhorst. In order to enable an isothermal experiment by avoiding temperature effects such as local warming or temperature gradients, care was taken that the incoming gas was cooled down before entering the sample cell.

This setup allowed for the change of the gas composition from pure CH_4 to a mixture containing 23 mol% CO_2 and 77 mol% N_2 at pressures between 6.9 and 9.1 MPa at 278 K after the initial CH_4 hydrate phase was formed. For the Raman measurements, a confocal Raman spectrometer (LABRAM, HORIBA) was used, which allowed for the laser beam to be focused on a precise spot, for example, the surface of a hydrate crystal, thus ensuring that only the selected phase was analyzed. The instrument parameters were the following: grating, 1800 grooves/mm; entrance slit, 100 μm; confocal pinhole, 100–200 μm; microscope objective, 20×; laser, external 100 mW diode-pumped solid-state laser with a wavelength of 532 nm. The Raman instrument was calibrated using silicon (521 cm^{-1}) and diamond (1,332 cm^{-1}). The accuracy of the spectrometer was determined with 3 cm^{-1} (Schicks & Luzi-Helbing, 2013).

2.2. Medium Scale Measurements Using Ex Situ X-Ray Diffraction and Raman Spectroscopy

For the experiments on a medium scale, we used pressure vessels with a volume of about 420 ml. Ice was prepared by spraying deionized water into liquid N_2. The ice beads were grinded in a cryo-mortar before 130 ml of ice beads or 100 ml of sand ($SiO_2 > 96\%$, 80–90% 0.5–1.0 mm), and 30 ml of ice beads were mixed in a beaker and filled into the pressure vessels, pressurized with CH_4 (8.0–10.0 MPa), and stored into a cooling box at 263–268 K for several weeks. A pressure drop at the beginning of the storage indicated the formation of CH_4 hydrate. After 6–9 weeks, no changes in pressure could be detected. Based on the pressure drop and the resulting moles of consumed CH_4, we roughly calculated the amount of ice transformed into hydrate, which was about 23% in case only ice were present and between 49% and 71% in case ice was mixed with sand. According to the shrinking core model (Kuhs et al., 2006), we assume that all ice particles are—depending on their diameter—at least covered with a CH_4 hydrate shell or completely transformed into CH_4 hydrate. At that point, CH_4 was exchanged with a gas mixture containing 23 mol% CO_2 and 77 mol% N_2. For this, the remaining/nonconverted CH_4 head space gas was released and instantly replaced by the CO_2-N_2 gas mixture. In line with the pressure conditions in the field trial, the applied pressures varied between 7.8 and 9.8 MPa. In four additional experiments, the pressure was chosen above the applied pressures in the field trial, between 10.2 and 11.3 MPa. After exchange of the gas phase, the vessels were stored in a cooling box at 278 K for 2 days. Thereafter, the gas phase was analyzed, and the vessels were opened. If present, the solid phase (including some water as a result of hydrate dissociation or ice melting) was recovered and stored in liquid nitrogen.

For Raman spectroscopic measurements, small pieces of the solid phase were transferred into a Linkam stage at 150 K and analyzed using the same Raman spectrometer described above.

Table 1
Overview of the Experimental Conditions

Cell type	Analysis	Cell volume	Sample	Pressure (MPa)	Temperature (K)
Flow-through pressure cell	In situ Raman spectroscopy	0.393 mL	150 μl water + gas	6.9–9.1	278
Batch reactor	Ex situ Raman spectroscopy and X-ray diffraction	420 mL	130 ml ice + gas or 30 ml ice +100 ml sand + gas	7.8–11.3	278
LARS	GC	210/425 L	210 L sediment + CH_4 saturated water	10	281

Note. LARS = LArge-scale Reservoir Simulator; GC = gas chromatography.

For the X-ray diffraction measurements, the sample material (hydrate + ice) was continuously handled in liquid nitrogen, and all preparation work was carried out in a cooled glove box at 263 K to minimize hydrate dissociation and condensation of air moisture onto the sample. The sample was grounded in a freezer mill (Spex CertiPrep). The fine crystalline hydrate/ice powder sample was immediately placed on a precooled copper sample holder in a low-temperature chamber (153 K) and measured at ambient pressure. The powder X-ray diffraction patterns were obtained with an Empyrean theta-theta system (PANalytical) with Cu K_α radiation (λ = 0.15406 nm) generated at 40 kV and 40 mA. The measurements were carried out in a continuous scan mode in the 2θ range of 8–55° with a total scan time of 312 s. The diffracted X-rays were detected with a PIXcel^{3D} detector. The spectra were computationally processed to evaluate the hydrate structure and the ratio of ice:hydrate using EVA v11.0.0.3 and AutoQuan v2.7.1.0, respectively.

Prior to the measurements of the ice/hydrate samples, the position of the sample stage was checked by measuring an ice sample. The peak positions of the ice reflections were compared with literature data for hexagonal ice using the program EVA (Rundle, 1953). The obtained powder pattern of the hydrate/ice samples were also referenced to ice Ih reflections using EVA. The present phases were quantified by means of Rietveld refinement using the full pattern Rietveld program AutoQuan (Kleeberg & Bergmann, 1998). The crystallographic data for hexagonal ice and structure I hydrate were obtained from the literature (Kirchner et al., 2004; Rundle, 1953; Yousuf et al., 2004). The refinement parameters were the phase fractions of ice and structure I hydrate, seven background parameters, and the lattice constants. The atomic positions and displacement parameters were fixed.

2.3. The LArge-Scale Reservoir Simulator (LARS)

The LARS is a worldwide unique setup in terms of size and operational parameter and designed for experimental simulations of reservoir-related processes on a pilot-plant scale. It has a total volume of 425 L and holds a sample volume of about 210 L. It allows for the formation of gas hydrates from CH_4-loaded brine in sediments at pressures up to 25 MPa. The LARS is equipped with a series of pressure and temperature sensors and a cylindrical electrical resistivity tomography (ERT) array composed of 375 electrodes. The ERT is used to monitor the formation and dissociation of gas hydrates and allows for the estimation of the hydrate saturation and distribution within the LARS. Detailed information about the LARS, the formation of CH_4 hydrates from CH_4-loaded brine, and the ERT are published elsewhere (Priegnitz et al., 2013, 2015; Spangenberg et al., 2015).

In this study CH_4 hydrates were formed in sand ($SiO_2 > 96\%$, 80–90% 0.5–1.0 mm) from CH_4 loaded brine at 281 K and a pore pressure of 10 MPa (confining pressure: 13 MPa) until the hydrate saturation reached about 70%. ERT measurements indicated a heterogeneous hydrate distribution in the sediments with a tendency to higher saturation toward the periphery of the sample reservoir.

A gas mixture of 23 mol% CO_2 and 77 mol% N_2 was injected from the bottom of the LARS. While the injection pump was flow controlled, the production pump was pressure controlled to keep the pore pressure of 10 MPa. The temperature was kept at 281 K and the confining pressure at 13 MPa. A total of six production periods were carried out, separated by shut-in periods of 20 hr to 11 weeks. The composition of the produced gas phase was analyzed for CH_4, N_2, and CO_2 using a two-channel gas analyzer CompactGC (Global Analyzer Solutions). The amount of produced water was determined by weighing. Table 1 summarizes all experiments and chosen conditions.

Table 2
Raman Bands and Assignments for the Studied Components in Gas and Hydrate Phases

Component	Hydrate/gas phase	$\nu_{measured}$ (cm^{-1})	$\nu_{literature}$ (cm^{-1})	Vibrational mode	Reference
CH_4	Gas phase	2,916	2,917	ν_1 C-H symmetric stretching	Subramanian and Sloan (1999)
	Structure I hydrate 5^{12}	2,915	2,915		
	Structure I hydrate $5^{12}6^2$	2,904	2,905		
CO_2	Gas phase	1,283	1,285	ν_1 C-O symmetric stretching	Burke (2001)
	Hydrate	1,275	1,274		Schicks et al. (2011)
	Gas phase	1,385	1,388	$2\nu_2$ overtone of bending	Burke (2001)
	Hydrate	1,379	1,377		Schicks et al. (2011)
N_2	Gas phase	2,328	2,331	ν_1 symmetric stretching	Burke (2001)
	Hydrate	2,323	2,324		Jin et al. (2015)

3. Results and Discussion

3.1. Results From In Situ Measurements on a Microscale Using Raman Spectroscopy

As mentioned in the previous section, CH_4 hydrate was formed from deionized water over several days until Raman measurements show characteristic spectra for CH_4 hydrate indicating an occupancy ratio of CH_4 encased in large and small cavities of structure I hydrate close to three (see also Figure 3b).

At this point, the pressure was adjusted to one specific pressure between 6.9 and 9.1 MPa, and the CH_4 gas phase was exchanged with the CO_2-N_2 gas mixture. Raman spectra were continuously taken to monitor the change of the composition of both, the gas phase and the hydrate phase. Table 2 gives a list of measured and assigned Raman band positions and the corresponding literature data. The position of the Raman bands is significantly shifted to lower wavenumbers when the component is encased in a hydrate lattice. This is true for all measured components CO_2, N_2, and CH_4 and allows for a clear differentiation between a component as part of the gas or hydrate phase. For the calculations of the composition of the gas and hydrate phases, the same routine was used as described in Beeskow-Strauch et al. (2011). The integrated band intensities were corrected with wavelength-independent cross-section factors, assuming that the cross section factors do not vary with pressure, cage type, or the overall composition of the phases (Burke, 2001; Schrader, 1995; Schrötter & Klöckner, 1979). Errors in the estimate of the concentration of one component based upon replicate analyses are ±2 mol%. The composition of the CH_4, CO_2, and N_2 in the gas and hydrate phase is given as relative percentage assuming that the corrected integrated intensities of the selected Raman bands for the molecules are set to 100%.

Independently from the chosen pressure, the initial CH_4 hydrate phase dissociated without any changes in composition over time when exposed to the CO_2-N_2 gas mixture. However, microscopic observation showed that with increasing pressure, the dissociation of the initial CH_4 hydrate proceeds slower: At 6.9 MPa, the decomposition of the initial hydrate phase was completed after 25 h, whereas CH_4 hydrate crystals remained after more than 60 hr at pressures $>$8.1 MPa. This pressure-dependent dissociation behavior of the CH_4 hydrate is depicted in Figure 1. The microscopically taken pictures show that most of the hydrate crystals were melted after 20 hr when the chosen pressure was 6.9 MPa at 278 K. The Raman spectra of the solid phase clearly indicate CH_4 hydrate and did not change until the dissociation process was quite advanced. In contrast, the hydrate crystals did not show significant changes under the microscope after 20 hr when the chosen pressure was $>$8.1 MPa at 278 K. Optical changes of the hydrate crystals could be observed after $>$48 hr, but the Raman spectra still indicate pure CH_4 hydrates even after 68 hr. At a higher absolute pressure, the system is deeper within the stability field of a simple CH_4 hydrate, which is a possible reason for a slower decomposition of the initial CH_4 hydrate. In addition, with increasing absolute pressure, the partial pressure of CH_4 in the gas phase increases, which also may affect the dissociation kinetics of the CH_4 hydrate phase.

In addition to the dissociation process, the concurrent formation of a secondary mixed hydrate phase besides the initial CH_4 hydrate phase was only observed at pressures $>$8.1 MPa. Microscopic observations indicate that the secondary hydrate phase grew as nuggets on the initial CH_4 hydrate phase as shown in Figure 2.

Raman spectra taken from the hydrate phases clearly showed the coexistence of the initial pure CH_4 hydrate phase besides a gas phase and a mixed hydrate phase containing CO_2, N_2, and CH_4. Figure 3 shows the corresponding Raman spectra of the mixed gas phase and the newly formed mixed hydrate phase at 278 K and

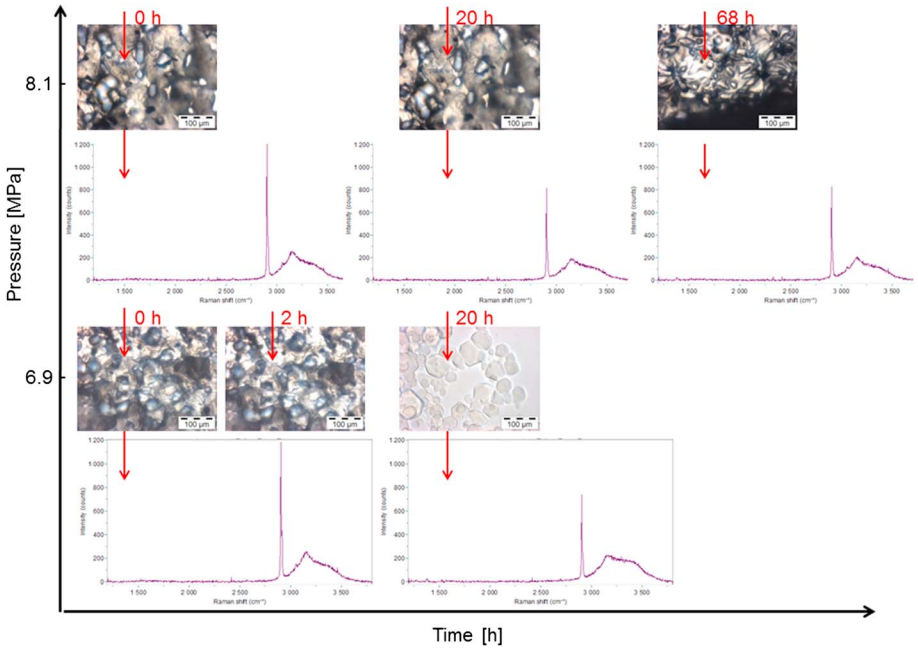

Figure 1. Pressure-dependent dissociation behavior of the initial CH_4 hydrate crystals when exposed to a CO_2-N_2 gas mixture. Microscopic observations indicate the dissociation of almost all hydrate crystals after 20 hr at 6.9 MPa and 278 K. At pressures >8.1 MPa and 278 K, no significant changes of the initial CH_4 hydrate crystals could be observed after 20 hr. After 68 hr, the shape and appearance of the initial CH_4 hydrate crystals have changed significantly; however, the Raman spectra still indicate a simple CH_4 hydrate phase.

pressures >8.1 MPa. The Raman spectrum of the coexisting initial CH_4 hydrate phase did not change over time. It is also shown in Figure 3.

The amounts of N_2, CO_2, and CH_4 encased in the secondary hydrate phase varied as shown in Figure 4. The composition was calculated from Raman spectra taken at different measuring points of the secondary formed hydrate phase. As a result of these calculations, the gas encased in the hydrate phase were composed of 5–30 mol% CH_4, 51–69 mol% CO_2, and 19–26 mol% N_2. The corresponding free gas phase at that time contained about 10 mol% CH_4, 21 mol% CO_2, and 69 mol% N_2. The results indicate an enrichment of CO_2 in the secondary formed hydrate phase compared to the initial gas phase (23 mol% CO_2 and 77 mol% N_2). CO_2 is

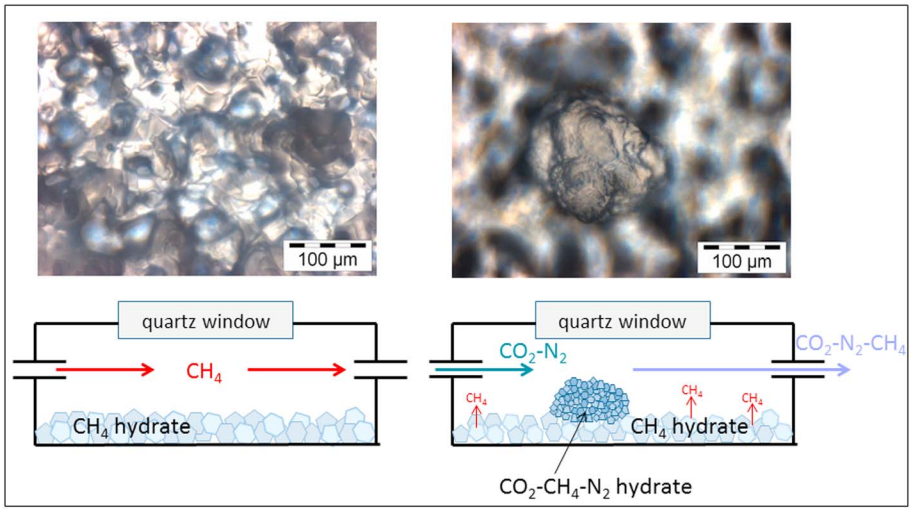

Figure 2. After the initial CH_4 hydrate phase was formed (left) and the gas phase was exchanged to a CO_2-N_2 mixture, the formation of a secondary mixed hydrate phase containing CO_2, N_2, and CH_4 on the initial CH_4 hydrate phase was observed at pressures >8.1 MPa and 278 K (right).

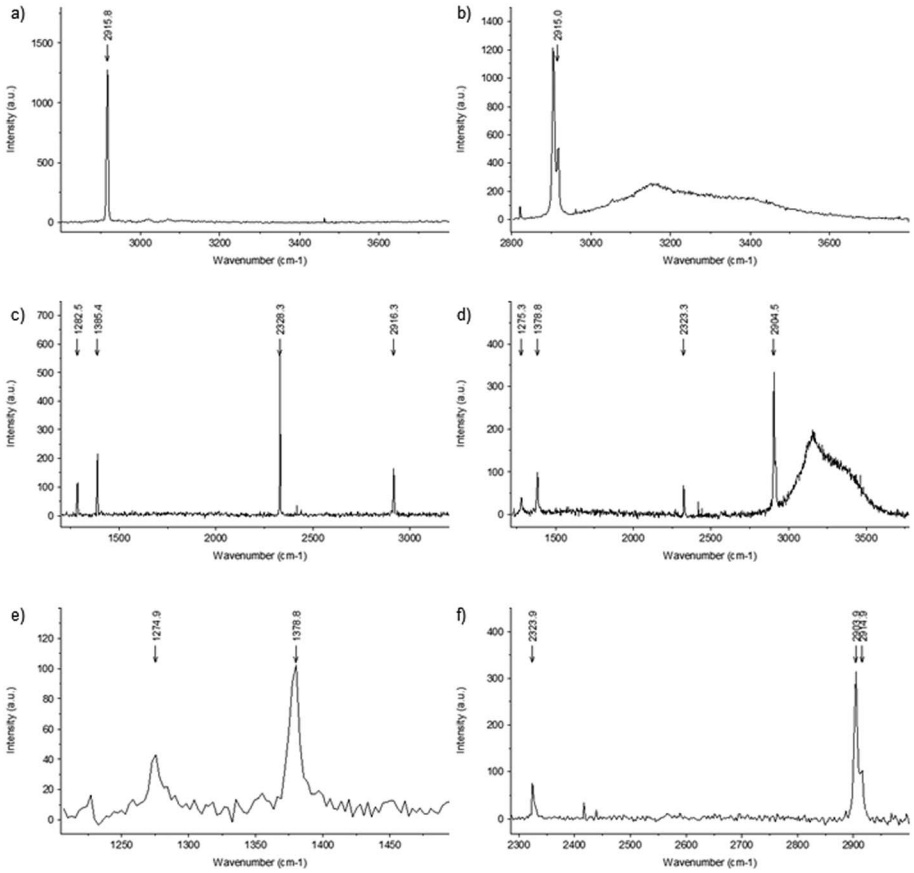

Figure 3. (a) Raman spectrum of the CH_4 gas phase; (b) Raman spectrum of pure CH_4 hydrate; (c) Raman spectrum of the gas phase after the change from CH_4 to a CO_2-N_2 mixture; (d) Raman spectrum of the newly formed secondary hydrate phase containing CO_2, N_2, and CH_4; (e) section of the Raman spectrum of the secondary hydrate: the position of the CO_2 bands at 1,275 and 1,379 cm^{-1} indicates the encasement of CO_2 in the hydrate phase; and (f) section of the Raman spectrum of the secondary hydrate: the position of the Raman bands for N_2 at 2,324 cm^{-1} and CH_4 at 2,904 and 2,915 cm^{-1} indicates the incorporation of N_2 and CH_4 into the hydrate structure.

known as a good hydrate former, and the enrichment of CO_2 in the hydrate phase has already been reported in a different context elsewhere (Schicks & Luzi-Helbing, 2015). Since N_2 is a small molecule and a comparably weak hydrate former (Sloan & Koh, 2008), the amount of N_2 encased in the hydrate phase is low compared to the amount of N_2 in the free gas phase. Nevertheless, for an achievement of an equilibrium state between the hydrate phase and the coexisting free gas phase, the encasement of all components of the free gas phase into the hydrate phase is essential. Therefore, we did not observe the formation of a pure CO_2 hydrate or a CO_2-N_2 hydrate. The ratio of large and small cavities occupied with CH_4 in the newly formed mixed hydrate phase varies between 1.7 and 3.6, indicating that there is no preference of CH_4 to occupy any type of cavities.

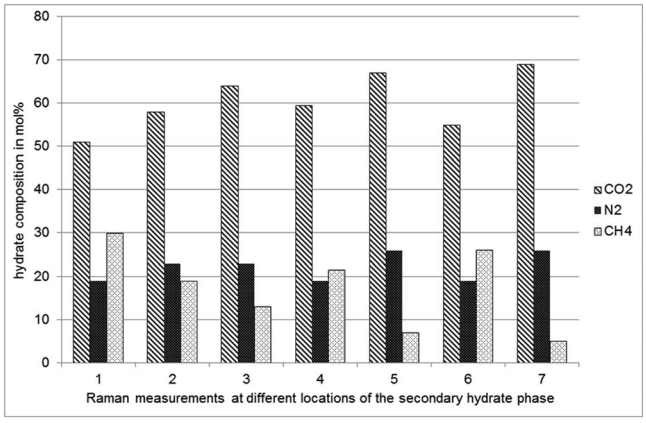

Figure 4. Compositions of the secondary formed hydrate phase containing various amounts of CO_2, N_2, and CH_4.

According to literature, the interactions between a CO_2 phase and an initial CH_4 hydrate phase are described as a replacement of the encased CH_4 molecules with CO_2 molecules: The process is divided into two steps. The first step is a fast reaction at the interface between the hydrate grain and the CO_2 fluid, where a partial destruction of the hydrate cavities and/or rearrangements of water molecules results in a fast release of CH_4 molecules (Falenty et al., 2016; Ota et al., 2005). According to Falenty et al. (2016), this destruction is limited to the

surface before new, mixed hydrate forms. The second step involves the much slower transport of the gas molecules through the bulk hydrate via diffusion (Ota et al., 2005) supported by empty cages in the hydrate structure as well as water vacancies in the cage walls (Falenty et al., 2016; Peters et al., 2008). Eventually, due to the rearrangement of cavity and guest molecules, the initial CH_4 hydrate phase is transformed into a CH_4-CO_2 mixed hydrate phase. Regarding the interactions between a CO_2-N_2 gas mixture and an initial CH_4 hydrate phase, Park et al. (2006) assumed an idealized cage-specific pattern of CO_2 and N_2, whereby N_2 molecules "attack" CH_4 molecules occupying 5^{12} cavities and CO_2 molecules replace most of the CH_4 molecules in $5^{12}6^2$. This specific exchange of the guest molecules in the hydrate phase results in mixed hydrate containing 23% N_2, 62% CO_2, and 15% CH_4 (Park et al., 2006; Shin et al., 2008).

In this study, however, the observed interaction between the initial CH_4 hydrate phase and the CO_2-N_2 gas mixture is different. Neither did we observe a fast surface reaction resulting in a release of CH_4 nor did we observe the incorporation of CO_2 or N_2 into the initial hydrate phase resulting in the formation of a mixed hydrate at the surface of the original hydrate grain. In contrast, we observed two parallel processes: (1) the relatively slow dissociation of the initial CH_4 hydrate phase showing only minimal changes of the habitus of the CH_4 hydrate crystals and (2) the formation of a new, mixed hydrate phase as nuggets on the initial CH_4 hydrate phase. These secondary formed hydrate nuggets contained CO_2 and N_2 as well as those CH_4 and H_2O molecules released due to the dissociation process of the initial CH_4 hydrate phase.

3.2. Results From Measurements on a Medium Scale Using Ex Situ X-Ray Diffraction and Raman Spectroscopy

After the exchange of the CH_4 gas phase with the CO_2-N_2 gas mixture, the pressure vessels were stored for 2–3 days in a cooling box at 278 K. The chosen pressures varied between 9.8 MPa, which corresponds to the injection pressure of the Iğnik Sikumi Field Trial, and 7.8 MPa, according to pressures likely occurring in the reservoir close to well bore. Thereafter, the gas phase was analyzed, and the pressure vessels were opened to recover the solid phase. The amount of CH_4 in the gas phase varied between 1.3 and 3.5 mol%, whereas the amount of CO_2 in the gas phase varied between 20.5 and 22.7 mol%. At pressures between 7.8 and 8.3 MPa, we could not recover a gas hydrate phase; the initial CH_4 hydrate phase was completely dissociated. At pressures $>$9.1 MPa, small amounts (up to 20%) of structure I hydrates in coexistence with ice could be detected in the solid phase using X-ray diffraction. Raman spectroscopic measurements specify a pure CH_4 hydrate with no indication of CO_2 or N_2 encased in the hydrate phase or the formation of a secondary mixed hydrate phase containing CH_4, CO_2, and N_2. These observations were independently if sand was present or not.

Interestingly, we could not observe the formation of a secondary mixed hydrate phase in the batch experiments at pressures 9.1–9.8 MPa at 278 K although these pressure and temperature conditions were within the stability field of the CO_2-N_2 and the CH_4-CO_2-N_2 mixed hydrate. Since the batch experiments were conducted in a pressure cell without any refreshment of the gas phase after the exchange of CH_4 with the CO_2-N_2 gas mixture, it can be considered as a closed system. Due to the chemical disequilibrium between the initial CH_4 hydrate phase and the coexisting CO_2-N_2 gas phase, the original hydrate phase dissociated and released CH_4, resulting in a gas mixture with low partial pressures for CH_4 and CO_2. The formation of a secondary mixed hydrate would result in a further depletion of CH_4 and in particular CO_2 in the gas phase, because the latter tends to be enriched into the hydrate phase. As a result, the partial pressure of CO_2 (and CH_4) in the gas phase is probably slightly too low for the formation of a hydrate phase or the amounts of formed hydrate are too small to be detected. In contrast, when we conducted the experiments using the continuous gas flow, the gas phase was refreshed every minute, and thus, the partial pressure of CO_2 in the gas phase remained constant, even during the formation of the secondary mixed hydrate phase. Therefore, we observed the formation of a secondary mixed hydrate phase already at pressures $>$8.1 MPa.

In addition to these experiments at pressures occurring at the field trial, we conducted four more experiments at medium scale applying pressures above 10 MPa. Two experiments were conducted with pure hydrate and two with a sediment/hydrate mixture (see section 2.2 for sample preparation). After CH_4 hydrates have formed, the CH_4 gas phase was exchanged with the CO_2-N_2 gas mixture, and the pressure vessels were stored for 3 days in the cooling box at 278 K. The pressures were chosen between 10.2 and 11.3 MPa. X-ray diffraction analyses of the recovered solid phase indicate up to 32% structure I hydrate

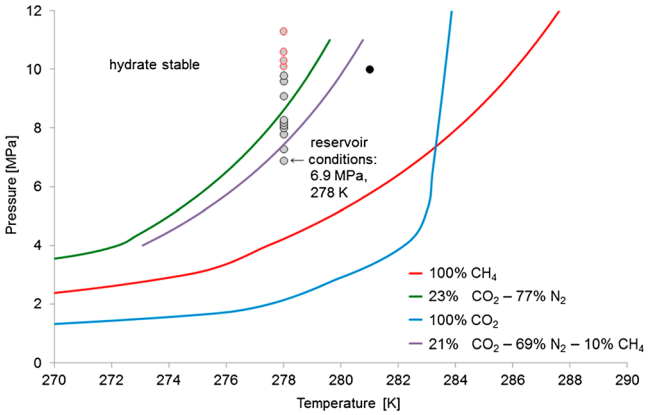

Figure 5. *p-T*-stability conditions for CH_4 hydrate (red), CO_2 hydrate (blue), a mixed hydrate formed from a feed gas mixture containing 23 mol% CO_2 and 77 mol% N_2 (green), and a mixed hydrate formed from a feed gas mixture containing 10 mol% CH_4, 21 mol% CO_2, and 69 mol% N_2 (purple). All stability limits were calculated with CSMGem (Sloan & Koh, 2008). The gray dots indicate the pressure and temperature conditions chosen for the microscale and medium scale experiments (gray dots with red frame indicate pressures above those pressures applied in the field trial), and the black dot indicates the pressure and temperature conditions chosen for the large-scale reservoir simulator experiment.

besides ice. Similar to the experiments conducted at pressures <9.8 MPa, the Raman spectroscopic measurements prove the existence of pure CH_4 hydrate. However, in contrast to the experiments conducted at pressures <9.8 MPa, we also detected mixed gas hydrates containing CO_2, N_2, and CH_4. These mixed hydrates were very heterogeneous regarding their composition: They contained up 18 mol% N_2. The amount of hydrate-bonded CO_2 in these newly formed hydrates varied between 9 and 60 mol% whereas the amount of CH_4 varied between 21 and 90 mol%. In the sample that experienced the highest pressure (11.3 MPa), we could also identify a mixed hydrate phase containing only CO_2 and N_2 but no detectable CH_4.

All microscale (flow-through) and medium (batch) scale experiments were conducted at pressure and temperature conditions within the CH_4 and the CO_2 hydrate stability fields (see Figure 5). Nevertheless, the results of our experiments clearly show that the initial CH_4 hydrate dissociated when exposed to the CO_2-N_2 gas mixture. Due to the changes of the chemical environment, the pure CH_4 hydrate did not remain. Remarkably, we could not observe an exchange of the CH_4 molecules in the original hydrate phase with CO_2 or N_2 molecules. Instead, we observed in the flow-through and the batch experiments the dissociation of the initial CH_4 hydrate on the one hand and the formation of a secondary mixed hydrate phase on the other hand. Since the new formed hydrate phase aimed to achieve a chemical equilibrium with the surrounding gas phase, this secondary hydrate phase contained CH_4, CO_2, and N_2 in varying quantities according to the composition of the gas phase. As expected, the formation of a pure CO_2 hydrate was not observed. In only one batch experiment applying a pressure of 11.3 MPa, we could detect a hydrate phase containing only CO_2 and N_2 but no CH_4, indicating that the system did not reach equilibrium.

During the Iġnik Sikumi Field Trial, a decreasing injectivity due to hydrate formation (of unknown composition) was observed in the early stages of the CO_2-N_2 injection period. Although the transferability to the field may be limited, the results of our microscale and medium scale experiments suggest that the hydrates that formed during the injection were mixed hydrates containing various amounts of CH_4, CO_2, and N_2. In our experiments, the formation of CO_2-N_2 hydrates could only be observed at 11.3 MPa, a pressure above the highest pressure that occurred in the field trial. As observed in our lab experiments, the changes of the chemical environment of the initial hydrate phase due to the CO_2-N_2 injection may also lead in the field to the dissociation of the native CH_4 hydrate phase and thus to a release of CH_4. Depending on the local pressure, a secondary mixed hydrate phase containing CH_4, CO_2, and N_2 may have formed.

3.3. Results From the LARS Experiment

The experiment in the LARS was conducted at 10 MPa and 281 K, which are conditions within the stability fields of CH_4 and CO_2 hydrate but out of the stability field of a CO_2-N_2 mixed hydrate (see black dot in Figure 5). The chosen *p-T* conditions avoid the formation of a secondary mixed hydrate with the pore brine, which may have resulted in clogging. With this approach, we preserved the injectivity during the injection of the CO_2-N_2 gas mixture. The CO_2-N_2 gas mixture was injected from the bottom of the pressure vessel with an initial flow rate of 50–100 ml/min. However, developments during the experiment made it necessary to adjust the injection rate. The initial average CH_4 hydrate saturation in the sandy sediment was 70% and according to ERT heterogeneously distributed (see also section 2.3).

Generally, the experiment can be divided in five daytime production periods (Figure 6) comprising gas injection and production from the reservoir. These times were interrupted by soaking periods of variable length, during which the sample reservoir was kept close to aim for an equilibrium or at least steady state. After a soaking phase of 11 weeks, a final production period was carried out by depressurization.

The gas composition measured during the first five production periods of the LARS experiment is shown in Figure 6. High N_2 and CO_2 concentrations were measured at the top of the sample reservoir already 20 min

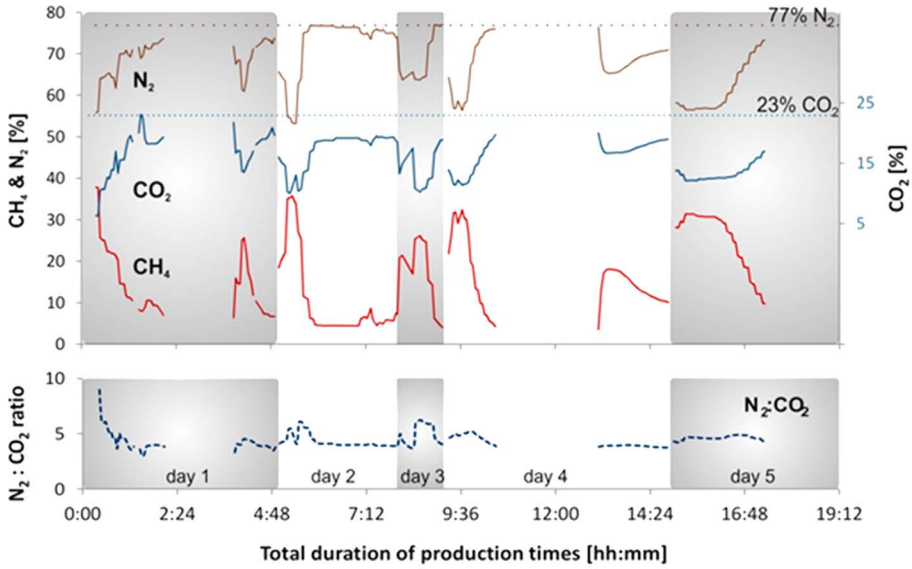

Figure 6. Composition of effluent gas (CH_4, CO_2, and N_2) during the large-scale reservoir simulator production test using a CO_2-N_2 mixture (23 mol% CO_2; 77 mol% N_2; indicated by dotted lines) to be injected into the reservoir. The compositions are shown as a function of the summated times of the five production periods excluding any equilibration periods when valves were closed (overnight from days 1–4 and for 120 hr between days 4 and 5). During production periods 1 and 4 (days 1 and 4), an interruption occurred, and the valves had to be closed for 1–2 hr (shown as data gaps).

after starting the injection of the gas mixture at the bottom. About 2 hr later, the N_2:CO_2 ratio in the effluent gas was close to that of the injected gas phase whereas the CH_4 concentration decreased. This indicated an immediate pathway of the injected gas, which preferably migrated through those areas with high permeability and hence low hydrate saturation. This in turn led to minor interaction between the initial CH_4 hydrate phase and the injected gas phase. Since little pore water was produced from the reservoir during day 1 (1.7 L) and day 2 (0.2 L), water was removed manually from the sample reservoir toward the end of injection periods 3 and 4 (1.4 and 2.4 L, respectively) when the CH_4 concentration in the effluent gas had decreased to 5–7 mol%. For this purpose, an additional port close to the bottom of the sample reservoir was used. This procedure increased the free gas volume in the sample reservoir and the contact area between gas, water, and hydrate phases. The effluent gas was dry and clogging had not been an issue throughout the experiment, indicating that pathways once formed stayed open.

The beginning of the production periods was characterized by high CH_4 concentrations (31–37 mol%) and elevated N_2:CO_2 ratios, both of them decreasing fast in periods 1 and 2. Also after short periods of short times of closure, a transient increase of CH_4 in the produced gas phase could be detected (production periods 1 and 4). In the short production period 3, the manual water discharge overlapped with the CH_4 production, extending it. As a consequence of the manual water removal, the volume of effluent gas with elevated CH_4 concentrations increased during production days 4 and 5. Following an extended soaking period (120 hr), the last production period (5) was characterized by the largest gas release.

The initial increase in CH_4 is a clear indicator for CH_4 hydrate decomposition throughout the soaking period, but the effect of the soaking time on this process seemed to be limited. These observations are in agreement with findings from Seo et al. (2015). They also observed a transient increase of CH_4 in the produced gas phase after each soaking period, whereas the soaking time does not change the amount of the produced CH_4.

The capture of CO_2 in the reservoir, evidenced by the increase in N_2:CO_2 ratios of the effluent gas, could be based on the higher solubility of CO_2 in water compared to N_2 (AirLiquid, 2009) as well as the preferential CO_2 incorporation in a mixed hydrate phase. The last mentioned corresponds to the observation made in our in situ Raman experiments. The gas composition of 30–35 mol% CH_4, 10–12 mol% CO_2, and 55 mol% N_2 measured at the beginning of each production period would be in equilibrium with a mixed hydrate stable up to 279.5 K at a given pressure of 10 MPa (CSMGem; Sloan & Koh, 2008). However, the chosen temperature in the

LARS was 281 K. Even an increase of CO_2 to 15 mol%, CH_4 to 35 mol%, and reducing N_2 to 50 mol%, thus, having accounted for a dilution by the injection of the N_2:CO_2 mix, would be a vapor mix in equilibrium with a structure I gas hydrate up to 280.8 K. Therefore, the formation of a mixed gas hydrate containing CO_2, N_2, and CH_4 at the given temperature and pressure condition was unlikely.

The analysis of the effluent gas during the depressurization of the sample reservoir 11 weeks after the fifth CO_2-N_2 injection period indicated the formation of a small amount of a mixed CO_2-CH_4 hydrate phase. During the second depressurization, the period was characterized by a strong simultaneous increase in CO_2 (35 mol%) and CH_4 (27 mol%) and decrease in N_2 (38 mol%) with a N_2:CO_2 ratio < 1 (data not shown) over a delimited time period of 30 min while pore pressure had dropped to 52 bar. While the depressurization continued, the CO_2 and N_2 amounts steadily dropped to <5 mol% and <3 mol%, respectively, and CH_4 increased to >90 mol%. The increase of CH_4 during this depressurization points toward the remaining CH_4 hydrate phases. There was no indication for the decomposition of a pure CO_2 hydrate when we reached pressure below the limit of pure CO_2 hydrate.

4. Summary and Conclusions

We conducted experiments in pressure cells from 0.393 ml to 425 L to simulate processes occurring during the Iğnik Sikumi Field Trial on different scales. We aimed to investigate the interactions between an initial CH_4 hydrate phase and a gas mixture containing 23 mol% CO_2 and 77 mol% N_2. In our experiments, we observed that these interactions strongly depend on the experimental condition (e.g., pressure and temperature) and operational implementation (continuous flow versus batch). The key findings are as follows:

1. The results from our measurements on a microscale and medium scale both indicate that the initial CH_4 hydrate phase dissociate when exposed to a gas mixture containing 23 mol% CO_2 and 77 mol% N_2 even though pressure and temperature conditions were chosen within the CH_4 hydrate stability limits. The driving force for this process is the disturbance of the chemical equilibrium between the coexisting phases. The kinetic of the dissociation process depended on the pressure condition at a given temperature in the system; with increasing pressure the dissociation process lasted longer. There was no indication for the replacement of CH_4 in the initial hydrate phase with CO_2 or N_2.
2. At pressures >8.0 MPa, the formation of a secondary mixed hydrate phase was observed in the in situ experiments on a microscale working with a continuous gas flow. Microscopic observations and Raman spectroscopic measurements indicated the formation of a secondary mixed hydrate containing CH_4, CO_2, and N_2 according to the composition of the free gas phase. Microscopic observations verify that this process was a new hydrate formation because the new hydrate phases formed as nuggets in coexistence with the initial CH_4 hydrate phase. It was clearly not a result of a replacement of the guest molecules in the initial CH_4 hydrate phase. The composition of the gases encased in the mixed hydrate phases was very heterogeneous and varied between 5–30 mol% CH_4, 51–69 mol% CO_2, and 19–26 mol% N_2, showing a strong enrichment of CO_2 into the hydrate phase.
3. In our medium scale batch experiments at pressures $\leq$9.8 MPa, we could only observe the dissociation of the initial CH_4 hydrate phase but no formation of a secondary mixed hydrate phase, even though the absolute pressure and temperature conditions were chosen within the stability field of a CO_2-N_2 mixed hydrate or a CH_4-CO_2-N_2 mixed hydrate. A possible explanation could be that the formation of the secondary hydrate causes a depletion of CH_4 and CO_2 in the free gas phase below a minimum concentration necessary for the formation and/or stabilization of a mixed hydrate. As a result, very small amounts of a secondary hydrate phase might have formed only temporarily or were not detected.
4. The results from the LARS experiment indicate the decomposition of the initial CH_4 hydrate phase due to the injection of the CO_2-N_2 mixture as well as the likely formation of a mixed CO_2-CH_4 hydrate phase. We observed a channel flow of injected gas through the sample. As a result, very limited surface area of the initial hydrate phase was in contact with the injected gas mixture during the first production periods. However, it is very likely that the release of CH_4 from the initial hydrate phase was the result of the dissociation of the hydrate phase, but it could also be induced by a replacement of the hydrate-bonded CH_4 with CO_2. Both reactions continued until a new chemical equilibrium or steady state between hydrate and coexisting fluid was established. Therefore, we always observed similar compositions of the first produced effluent gas with a temporary high content of CH_4 after a shut-in soak period.

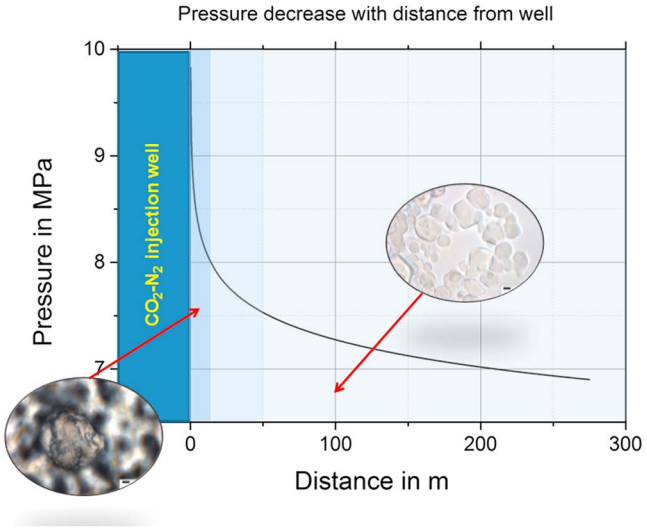

Figure 7. Pressure gradient depending on the distance from injection well. With increasing distance from the injection well, the pressure decreases, and the response of the hydrate in the sediments to the CO_2-N_2 injection is different. In the direct vicinity of the injection well, the formation of a secondary mixed hydrate is possible; at all other positions, the dominant process is the decomposition of the initial hydrate phase.

5. The measured composition of the gas produced during the depressurization test in the LARS indicated that a mixed hydrate containing CH_4 and CO_2 formed. There was no indication for the formation of a simple CO_2 hydrate or a CO_2-N_2 mixed hydrate.

The transferability of these findings to the Iġnik Sikumi Field Trial is limited. However, based on our experimental simulations, we suggest the following hypothesis: The response of the native CH_4 hydrate phase to the injection of the CO_2-N_2 mixture changes with the distance from the injection well. In the direct vicinity of the injection well, the pressure is high (>8.0 MPa), and the repeated injection of the CO_2-N_2 gas mixture refreshes the composition of the fluid phase. At these conditions, the formation of a secondary hydrate phase containing CO_2, N_2, and CH_4 is possible. At a larger distance (>50 m), the pressure in the reservoir decreases below 7.5 MPa, and the concentration of the injected CO_2-N_2 gas mixture decreases. Therefore, only the dissociation of the CH_4 hydrate phase but no formation of a secondary mixed hydrate phase occurs. In between, the secondary hydrate formation will be inhomogeneous and highly variable, dependent on the availability of fluid pathways and the local composition of the fluid phase. Figure 7 displays the different processes occurring at different distances from the injection well.

In conclusion, we assume that the dominant process of CH_4 gas release in the Iġnik Sikumi Field Trial was the straightforward dissociation of the native CH_4 hydrate due to changes of chemical equilibrium and aided by pressure reduction. An exchange reaction of the hydrate-bonded CH_4 with CO_2 and N_2 is unlikely. The injectivity decrease observed in the field test is likely due to the formation of a secondary mixed hydrate containing CO_2, N_2, and CH_4. Nevertheless, the addition of N_2 avoids fast secondary CO_2 hydrate formation along with blocking of pores space, which improves gas transport through the reservoir.

Acknowledgments
The authors thank Anja Schleicher and Martin Zimmer for the technical support during X-ray diffraction and gas chromatography measurements, respectively. We also thank the staff of the GFZ workshops for the construction of the pressure cells. The authors also gratefully acknowledge financial support from the German Federal Ministry for Economic Affairs and Energy and the German Federal Ministry of Education and Research within the project SUGAR (research grants 03SX320E and 03G0856C, respectively).

References

AirLiquid (2009). *1x1 der Gase–Physikalische Daten für Wissenschaft und Praxis* (4th ed.) Düsseldorf: Air Liquid Deutschland GmbH.

Beeskow-Strauch, B., Schicks, J. M., Spangenberg, E., & Erzinger, J. (2011). The influence of SO_2 and NO_2 impurities on CO_2 gas hydrate formation and stability. *Chemistry - A European Journal*, *17*(16), 4376–4384. https://doi.org/10.1002/chem.201003262

Boswell, R., Schoderbek, D., Collett, T. S., Ohtsuki, S., White, M., & Anderson, B. J. (2017). The Iġnik Sikumi Field Experiment, Alaska North Slope: Design, operations, and implications for CO_2−CH_4 exchange in gas hydrate reservoirs. *Energy & Fuels*, *31*(1), 140–153. https://doi.org/10.1021/acs.energyfuels.6b01909

Burke, E. A. J. (2001). Raman microspectrometry of fluid inclusions. *Lithos*, *55*(1-4), 139–158. https://doi.org/10.1016/S0024-4937(00)00043-8

Dallimore, S. R., & Collett, T. S. (2005). Summary and implications of the Mallik 2002 gas hydrate production research well program. Scientific results from Mallik 2002 gas hydrate production research well program, Mackenzie Delta Northwest Territories, Canada; Geological Survey of Canada, Natural Resources Canada: Ottawa, Ontario, Canada.

Deusner, C., Bigalke, N., Kossel, E., & Haeckel, M. (2012). Methane production from gas hydrate deposits through injection of supercritical CO_2. *Energies*, *5*(7), 2112–2140. https://doi.org/10.3390/en5072112

Falenty, A., Qin, J., Salamatin, A. N., Yang, L., & Kuhs, W. F. (2016). Fluid composition and kinetics of the in situ replacement in CH_4-CO_2 hydrate system. *Journal of Physical Chemistry C*, *120*(48), 27,159–27,172. https://doi.org/10.1021/acs.jpcc.6b09460

Hirohama, S., Shimoyama, Y., Wakabayashi, A., Tatsuta, S., & Nishida, N. J. (1996). Conversion of CH_4-hydrate to CO_2-hydrate in liquid CO_2. *Journal of Chemical Engineering of Japan*, *29*(6), 1014–1020. https://doi.org/10.1252/jcej.29.1014

Jin, Y., Kida, M., & Nagao, J. (2015). Structural characterization of structure H (sH) clathrate hydrates enclosing nitrogen and 2,2-dimethylbutane. *Journal of Physical Chemistry C*, *119*(17), 9069–9075. https://doi.org/10.1021/acs.jpcc.5b00529

Kang, S.-P., Lee, H., Lee, C.-S., & Sung, W.-M. (2001). Hydrate phase equilibria of the guest mixtures containing CO_2, N_2 and tetrahydrofuran. *Fluid Phase Equilibria*, *185*(1-2), 101–109. https://doi.org/10.1016/S0378-3812(01)00460-5

Kirchner, M. T., Boese, R., Billups, W. E., & Norman, L. R. (2004). Gas hydrate single-crystal structure analyses. *Journal of the American Chemical Society*, *126*(30), 9407–9412. https://doi.org/10.1021/ja049247c

Kleeberg, R., & Bergmann, J. (1998). Quantitative Röntgenphasenanalyse mit den Rietveld-Programmen BGMN und AUTOQUANT in der täglichen Laborpraxis. *Berichte der DTTG eV. Band*, *6*, 237–250.

Koh, D.-Y., Kang, H., Kim, D.-O., Park, J., Cha, M., & Lee, H. (2012). Recovery of methane from gas hydrates intercalated within natural sediments using CO_2 and a CO_2/N_2 gas mixture. *ChemSusChem*, *5*(8), 1443–1448. https://doi.org/10.1002/cssc.201100644

Kuhs, W. F., Staykova, D. K., & Salamatin, A. N. (2006). Formation of methane hydrate from polydisperse ice powders. *The Journal of Physical Chemistry. B*, *110*(26), 13,283–13,295. https://doi.org/10.1021/jp061060f

Kvamme, B., Graue, A., Buanes, T., Kuznetsova, T., & Ersland, G. (2007). Storage of CO_2 in natural gas hydrate reservoirs and the effect of hydrate as an extra sealing in cold aquifers. *International Journal of Greenhouse Gas Control*, *1*(2), 236–246. https://doi.org/10.1016/S1750-5836(06)00002-8

Kvenvolden, K.A., & T. D. Lorenson (2001). The global occurrence of natural gas hydrates. In C. K. Paull & W. P. Dillon (Eds.), *Natural gas hydrates–Occurrence, distribution and detection*, *Geophysical Monograph* (Vol. 124, pp. 3–18). Washington, DC: American Geophysical Union.

Lee, H., Seo, Y., Seo, Y.-T., Moudrakovski, I. L., & Ripmeester, J. (2003). Recovering methane from solid methane hydrate with carbon dioxide. *Angewandte Chemie, International Edition*, *42*(41), 5048–5051. https://doi.org/10.1002/anie.200351489

Ota, M., Abe, Y., Watanabe, M., Smith Jr, R. L., & Inomata, H. (2005). Methane recovery from methane hydrate using pressurized CO_2. *Fluid Phase Equilibria*, *228-229*, 553–559. https://doi.org/10.1016/j.fluid.2004.10.002

Park, Y., Kim, D.-Y., Lee, J.-W., Huh, D.-G., Park, K.-P., Lee, J., & Lee, H. (2006). Sequestering carbon dioxide into complex structures of naturally occurring gas hydrates. *Proceedings of the National Academy of Sciences of the United States of America*, *103*(34), 12,690–12,694. https://doi.org/10.1073/pnas.0602251103

Peters, B., Zimmermann, N. E. R., Beckham, G. T., Tester, J. W., & Trout, B. L. (2008). Path sampling calculation of methane diffusivity in natural gas hydrates from water-vacancy assisted mechanism. *Journal of the American Chemical Society*, *130*(51), 17,342–17,350. https://doi.org/10.1021/ja802014m

Priegnitz, M., Thaler, J., Spangenberg, E., Rücker, C., & Schicks, J. (2013). A cylindrical electrical resistivity tomography array for three-dimensional monitoring of hydrate formation and dissociation. *The Review of Scientific Instruments*, *84*(10), 104502. https://doi.org/10.1063/1.4825372

Priegnitz, M., Thaler, J., Spangenberg, E., Schicks, J., Schrötter, J., & Abendroth, S. (2015). Characterizing electrical properties and permeability changes of hydrate bearing sediments using ERT data. *Geophysical Journal International*, *202*(3), 1599–1612. https://doi.org/10.1093/gji/ggv245

Rundle, R. E. (1953). The structure and residual entropy of ice. *The Journal of Chemical Physics*, *21*(7), 1311. https://doi.org/10.1063/1.1699206

Schicks, J. M., Luzi, M., & Beeskow-Strauch, B. (2011). The conversion process of hydrocarbon hydrates into CO_2 hydrates and vice versa: Thermodynamic considerations. *The Journal of Physical Chemistry. A*, *115*(46), 13,324–13,331. https://doi.org/10.1021/jp109812v

Schicks, J. M., & Luzi-Helbing, M. (2013). Cage occupancy and structural changes during hydrate formation from initial stages to resulting hydrate phase. *Spectrochimica Acta Part A: Molecular and Biomolecular Spectroscopy*, *115*, 528–536. https://doi.org/10.1016/j.saa.2013.06.065

Schicks, J. M., & Luzi-Helbing, M. (2015). Kinetic and thermodynamic aspects of clathrate hydrate nucleation and growth. *Journal of Chemical & Engineering Data*, *60*(2), 269–277. https://doi.org/10.1021/je5005593

Schicks, J. M., & Ripmeester, J. A. (2004). The coexistence of two different methane hydrate phases under moderate pressure and temperature conditions: Kinetic versus thermodynamic products. *Angewandte Chemie, International Edition*, *43*(25), 3310–3313. https://doi.org/10.1002/anie.200453898

Schoderbeck, D., Farrell, H., Hester, K., Howard, J., Raterman, K., Silpngarmlert, S., et al. (2013). ConocoPhillips gas hydrate production test final technical report, US DOE/NETL Final Report.

Schrader, B. (1995). *Infrared and Raman spectroscopy*. Weinheim: VCH Verlagsgesellschaft mbH. https://doi.org/10.1002/9783527615438

Schrötter, H. W., & Klöckner, H. W. (1979). In A. Weber (Ed.), *Raman spectroscopy of gases and liquids* (pp. 123–166). Berlin: Springer-Verlag. https://doi.org/10.1007/978-3-642-81279-8_4

Seo, Y.-j., Kim, D., Koh, D.-Y., Lee, J. Y., Ahn, T., Kim, S.-J., et al. (2015). Soaking process for the enhanced methane recovery of gas hydrates via CO_2/N_2 gas injection. *Energy & Fuels*, *29*, 8143–8150. https://doi.org/10.1021/acs.energyfuels.5b02128

Sfaxi, I. B. A., Belandria, V., Mohammadib, A. H., Lugo, R., & Richon, D. (2012). Phase equilibria of CO_2 + N_2 and CO_2 + CH_4 clathrate hydrates: Experimental measurements and thermodynamic modelling. *Chemical Engineering Science*, *84*, 602–611. https://doi.org/10.1016/j.ces.2012.08.041

Shin, K., Park, Y., Cha, M., Park, K.-P., Huh, D.-G., Lee, J., et al. (2008). Swapping phenomena occurring in deep-sea gas hydrates. *Energy & Fuels*, *22*(5), 3160–3163. https://doi.org/10.1021/ef8002087

Sloan, E. D., C. A. Koh (2008). *Clathrate hydrates from natural gases*. Boca Raton, London, New York: CRC Press, Taylor and Francis Group.

Spangenberg, E., Priegnitz, M., Heeschen, K., & Schicks, J. (2015). Are laboratory-formed hydrate-bearing systems analogous to those in nature? *Journal of Chemical & Engineering Data*, *60*(2), 258–268. https://doi.org/10.1021/je5005609

Subramanian, S., & Sloan, E. D. (1999). Molecular measurements of methane hydrate formation. *Fluid Phase Equilibria*, *158-160*, 813–820. https://doi.org/10.1016/S0378-3812(99)00134-X

Yamamoto, K., Terao, Y., Fujii, T., Ikawa, T., Seki, M., Matsuzawa, M., & Kanno, T. (2014). Operational overview of the first offshore production test of methane hydrates in the Eastern Nankai Trough. Proceedings of the Offshore Technology Conference; Houston, TX, May 5–8, 2014. https://doi.org/10.4043/25243-MS

Yousuf, M. S., Qadri, B., Knies, D. L., Grabowski, K. S., Coffin, R. B., & Pohlman, J. W. (2004). Novel results on structural investigations of natural minerals of clathrate hydrates. *Applied Physics A: Materials Science & Processing*, *78*(6), 925–939. https://doi.org/10.1007/s00339-003-2091-y

Zhao, J., Xu, K., Song, Y., Liu, W., Lam, Y., Liu, K., et al. (2012). A review on research on replacement of CH_4 in natural gas hydrates by use of CO2. *Energies*, *5*(2), 399–419. https://doi.org/10.3390/en5020399